SUPPLEMENTARY INFORMATION

Asf1b, the necessary Asf1 isoform for proliferation, is predictive of outcome in breast cancer

Authors:

CORPET Armelle[1,2], DE KONING Leanne[1,2], TOEDLING Joern[1,2,3,4], SAVIGNONI Alexia[3,4], BERGER Frédérique[3,4], LEMAÎTRE Charlène[1,2], O'SULLIVAN Roderick J.[6], KARLSEDER Jan[6], BARILLOT Emmanuel[3,4], ASSELAIN Bernard[3,4], SASTRE-GARAU Xavier[5] and ALMOUZNI Geneviève[1,2*].

Affiliations:

1 Institut Curie, UMR218, Paris, F-75248 France.

2 CNRS, UMR218, Paris, F-75248 France.

3 Institut Curie, U900, Paris, F-75248 France.

4 INSERM, U900, Mines Paris-Tech, Paris, F-75248 France.

5 Institut Curie, Department of Pathology, Paris, F-75248 France.

6 The Salk Institute for Biological Studies. Molecular and Cellular Biology Dept. La Jolla, CA92037, USA.

* Corresponding author: Geneviève Almouzni: geneviève.almouzni@curie.fr, +33 1 56 24 67 01.

Supplementary Materials and Methods

Synchronization of cells

We synchronized BJ primary cells and U-2-OS osteosarcoma cells in quiescence by incubation in a serum-free medium for 72h, and MCF7 cells in medium containing 10nM of the anti-estrogen ICI182780 (Fisher Bioblock Scientific) (Carroll et al, 2000) for 48h. We synchronized HeLa cells with a double thymidine block, as follows: 16h block in 2,5mM thymidine (Sigma-Aldrich), 9h release in 30μM 2'-deoxycytidine (Sigma-Aldrich), and 16h block in 2,5mM thymidine. We collected the G1/S, S, S/G2, and G1 samples after a 0-, 4-, 8-, 14-h release in 30μM 2'-deoxycytidine respectively. We treated HeLa cells with 100ng/mL nocodazole for 15h to obtain mitotic samples.

We verified cell synchronization by flow cytometry, using cells fixed in 70% ethanol (-20°C) and stained with propidium iodide (50μg/mL in PBS containing 0,04mg/mL RNase A). We used a BD FACScalibur (BD Biosciences) for signal analysis and carried analysis with FlowJo (Tree Star Inc.) software.

Plasmid constructions

We generated N-terminal fusions of the C-Terminal part of Asf1b (amino-acids 156-202) to a GST-tag and to a His-tag by PCR cloning of the C-terminus of Asf1b (primers: 5'AGGTGCTAGAATTCAACATGGACAGGCTGGAGGCCATAG, 3'CAGGCTATCTCGAGTTATTAGATGCAGTCCATGGAGTTCTCAG), insertion into the EcoRI/XhoI site of pGEX-4T-1(Novagen) and pET-30a (Novagen) respectively followed by verification by sequencing. We generated N-terminal fusion of the C-Terminal part of Asf1a (amino-acids 156-204) to the His-tag by PCR cloning of the C-terminus of Asf1a (primers: 5'AGGTGCTAGAATTCAACACAGAAAAACTGGAAGATG, 3'CAGGCTATCTCGAGTTATCACATGCAGTCCATGTGGGATTC), insertion into the EcoRI/XhoI site of pET-30a (Novagen) and verification by sequencing.

Antibodies

Rabbit polyclonal antibody raised against the full-lenght GST-Asf1a (antibody #28134) was described previously (Mello et al, 2002). We produced an additional specific antibody against Asf1b. For this, we cloned the C-terminal part (amino-acids 156-202) of Asf1b in a pGEX-4T-1 vector (Novagen) (see above). For the immunization of two rabbits (#18130 and #18143) (Agrobio), we used bacterially expressed GST-C-Term-Asf1b recombinant protein

in *E. Coli* BL21 (DE3, Novagen) (Moggs et al, 2000), purified on glutathione beads (17-0756-01, GE Healthcare) and eluted with 10mM glutathione according to the manufacturer's instructions. We verified the specificity of both Asf1a and Asf1b antibodies as described in Supplementary Figure S1. Supplementary Table SI lists all primary antibodies used in this study with their source, reference, and dilutions for western blotting or immunofluorescence.

Immunofluorescence microscopy

Cells grown on coverslips, fixed in 2% paraformaldehyde, and permeabilized in PBS containing 0,2% Triton X-100, were processed as in (Martini et al, 1998). For lamin A staining, a pre-extraction step was performed to remove soluble proteins. Briefly, cells were washed with CSK, extracted with CSK 0.5% Triton X-100 and rinsed with CSK and PBS before fixation as described above. We used cross-absorbed Alexa-488 or Alexa-594 conjugated secondary antibodies (Molecular probes-Invitrogen) to detect primary antibodies (Supplementary Table SI). We acquired images with a DM600 (Leica) upright widefield epifluorescence microscope (63X objective/NA 1.32 or 40X objective/NA 1.0) piloted with Metamorph software and equipped with a chilled CCD camera (CoolSnap Hq2, Photometrics). We applied identical settings and the same contrast adjustment for all images to allow accurate data comparison, except for LaminA staining on Figure 4C which was specifically enhanced in Asf1b depleted cells in order to visualize the DNA bridges. For brightness and contrast adjustment, we used Adobe Photoshop CS3 (Adobe). For quantitative analysis, a minimum number of n=100 nuclei were counted per experiment.

RNA extraction and Quantitative RT-PCR

We performed all reverse transcription using Superscript II reverse transcriptase (Invitrogen) with 500ng-1μg of RNA and 300ng-3μg of random primers (Invitrogen) per reaction respectively. For quantitative PCR analysis, we used the 96-well plate Step One Plus system (Applied Biosystems) and the SYBR Green PCR Master mix (Applied Biosystems) or the KAPA SYBR® FAST ABI Prism® 2X qPCR Master Mix (KAPA Biosystems) and filled plates using an EpMotion 5070 Robot (Eppendorf). We measured duplicates in all experiments and checked the efficiency of each primer pair (sequences below) with three subsequent cDNA dilutions for each of the breast tumor samples. For each gene, we normalized the quantity of mRNA to the quantity of mRNA corresponding to the human acidic ribosomal phosphoprotein PO (RPLPO) (de Cremoux et al, 2004) or to the Glyceraldehyde 3-phosphate dehydrogenase (GAPDH). To compare with our transcriptome

analysis, we plotted mRNA levels relative to control siRNA levels and took logarithmic 2 values. This is referred to as the log2(fold change).

Primers

For analysis of the 86 and 71 breast tumor samples from 1995 and 1996 respectively, we used the following primers: Asf1a Forward: CAGATGCAGATGCAGTAGGC; Asf1a Reverse: CCTGGGATTAGATGCCAAAA; Asf1b Forward: GGTTCGAGATCAGCTTCGAG; Asf1b Reverse: CATGGTAGGTGCAGGTGATG; CAF-1 p60 Forward: CGGACACTCCACCAAGTTCT; CAF-1 p60 Reverse: CCAGGCGTCTCTGACTGAAT; CAF-1 p150 Forward: CAGCAGTACCAGTCCCTTCC; CAF-1 p150 Reverse: TCTTTGCAGTCTGAGCTTGTTC; RPLPO Forward: GGCGACCTGGAAGTCCAACT; RPLPO Reverse: CCATCAGCACCACAGCCTTC; GAPDH Forward: GAGTCAACGGATTTGGTCGT; GAPDH Reverse: TTGATTTTGGAGGGATCTCG. All other primer sequences used are available upon request.

Western blot quantification by chemiluminescence

For quantification, we performed acquisition of the chemiluminescence signal on a ChemiDoc XRS (BioRad) geldoc, and quantification of the intensity of the bands with Quantity One 4.6.6 software. We checked that the signal response is in a linear range using dilution series. We normalized values obtained for Asf1a or Asf1b levels to the levels of α-tubulin, or to the Memcode (Invitrogen) protein staining in the case of the mammary cell lines.

Transcriptome analysis

We used the package arrayQualityMetrics (Kauffmann et al, 2009) of the Bioconductor Project (Gentleman et al, 2004) for quality assessment to check for artifacts and quality issues with the eight arrays. For preprocessing, we downloaded the chip description file for this platform from the database of the University of Michigan (URL: http://brainarray.mbni.med.umich.edu/Brainarray/Database/CustomCDF/genomic_curated_CDF.asp). This chip description file consists of a single probe set each for 17,426 human genes annotated in the Ensembl database (Birney et al, 2004), and disregards probes that show potential cross-hybridization to transcripts of other genes. These alternate chip description files have been shown to outperform the standard chip description files supplied by the array manufacturer (Dai et al, 2005). We normalized and log-transformed the probe intensities

using the Bioconductor package vsn (Huber et al, 2002); we summarized the transformed probe intensities into gene (probe set) expression values using Tukey's median-polish procedure.

We determined differentially expressed genes using the Bioconductor package limma (Smyth, 2004). For each gene, we constructed a linear model that relates the expression value of the gene in the eight samples to a common intercept, an effect for the presence of the siRNA against Asf1a (siAsf1a) and an effect for the presence of the siRNA against Asf1b (siAsf1b). For each gene, a one-sample t-test was used to determine if the effects of siAsf1a and/or siAsf1b were significantly different from zero. For each test the variance of the gene term was shrunk towards an overall variance using the Empirical Bayes procedure of the Bioconductor package limma. We corrected the significant *p*-values of the t-tests for multiple testing by controlling the False Discovery Rate (Benjamini et al, 2001). We report an effect as significantly different from zero if the corrected *p*-value of the test was less or equal 0.05. Of note, we did not find any obvious conservation of our transcriptomic data with the one obtained in yeast (data not shown) suggesting that, beside sharing common molecular properties, human Asf1 isoforms and yeast Asf1 might have distinct functions.

To investigate whether the resulting lists of differentially expressed genes had significant association with Gene Ontology terms (Ashburner et al, 2000), we used the Bioconductor package topGO (Alexa et al, 2006). We obtained the Gene Ontology (GO) annotation of genes on the microarray from the Ensembl database in March 2009. We disregarded the associations between genes and GO terms which were solely inferred from electronic annotation (GO evidence terms: IEA, NAS, ND). To mitigate the dependencies between the tests imposed by the structure of the GO, if a gene was counted for the annotation of a specific gene, it was not counted again for any ancestor terms of this term ("elim" method of the package topGO). For each term, we performed a Hypergeometric test to determine whether genes of that list showed a more frequent association with a certain term than would be expected by chance given the GO annotation of all genes represented on the microarray. When the test resulted in a *p*-value inferior to 5.10^{-4}, we considered these terms as significantly over-represented for the given list.

In addition, we investigated the expression of Asf1a and Asf1b in another expression microarray data set. The data set consisted of breast cancer samples selected from the Institut Curie Human Tumor cryopreserved database. Breast cancer subtypes were selected based on their immunophenotype: Estrogen-Receptor (ER) positive for the luminal A subtype, ER positive and Grade III or ERBB2 positive for the luminal B subtype, ERBB2 positive for the

ERBB2 subtype, and triple negative for the basal-like subtype. The molecular phenotypes were determined on fixed samples and diagnosed at Institut Curie. Transcriptomic data of these samples were also obtained using the Affymetrix HGU133Plus2 microarray platform. We performed quality assessment and preprocessing of this data set as described above. We performed comparisons of the expression levels of Asf1a and Asf1b between sample groups by using two-sample Wilcoxon rank-sum tests. We corrected significant *p*-values ($p \leq 0.05$) of these tests for multiple testing using the Bonferroni method.

Breast tumor samples and statistics

We used samples from patients of 1995 with breast tumor classified as non-palpable (T0) or small (T1-T2) selected at the Institut Curie Biological Resources Center and treated with primary conservative tumorectomy (median tumor size: 18mm, range: 6-50mm). 92 patients diagnosed in 1995 and found to be lymph node negative (N0) and metastasis free (M0) granted permission to use their sample and data for research purposes. The median follow-up of the patients was 146 months (range: 30-161 months). Recurrence-free and alive patients were censored to the date of their last known contact. At the date of the analysis, 11% of the patients were no longer alive, with cause of death being the initial breast cancer in 70% of these cases. 10% of patients developed loco-regional recurrence and 15% developed metastasis. In addition, to confirm results obtained on the first set of tumors from 1995, we included a second independent set of patient samples from 1996 similar on all points to the first set. Patients and tumor characteristics are shown in Table SII and Supplementary Figure S8B.

We selected RNA extracted from 86 (set of 1995) or 71 (set of 1996) cryofrozen tissue of sufficient quality for analysis by RT-QPCR. For each gene, we expressed the quantity x of the gene mRNA relative to the quantity of RPLPO mRNA in a given sample by applying x=100*(E^(Cp RPLPO - Cp Gene)), where E is the mean efficiency of the primers. For statistical analysis, we retained data from 55 patients (1995) for Asf1a, 85 (1995) or 69 patients (1996) for Asf1b, 75 (1995) or 70 patients (1996) for CAF-1 p60 and 86 (1995) or 71 (1996) patients for CAF-1 p150 which fulfilled our amplification criteria (reproducible duplicates, consistent primer efficiency between samples). Importantly, because of the difference in the number of patients with data for Asf1a and for Asf1b, we verified that there was no significant differences in the composition of the two populations of patients (data not shown).

We calculated correlations between various factors using the Pearson correlation coefficient method and analysed differences between groups with the Kruskal-Wallis test for continous variables. The disease-free interval is defined as the time from the diagnosis of breast cancer until the occurence of disease progression, meaning local recurrence in the treated breast, regional recurrence in lymph node-bearing areas, controlateral breast cancer or distant recurrences (metastasis). We determined a cut-off value that is prognostic for the disease free interval (DFI) by using a Cox proportional risks model and used the Wald test to evaluate the prognostic value of this variable on each event. We estimated the overall survival (OS), the metastasis-free interval and the DFI rates using the Kaplan-Meier method and compared the values between groups using a log-rank test. We carried out a multivariate analysis to assess the relative influence of certain prognostic factors (age, number of mitosis, grade, estrogen and progesteron-receptor status as well as p60, p150, HP1α, Asf1b, Ki67 expression levels) on OS, DFI and metastasis free interval using the Cox stepwise forward procedure (Cox 1972). The significance level was 0.05. We used the statistical software R (2.5.0 version) for our analyses.

Supplementary Figure legends

Supplementary Figure S1: Specificity of Asf1 antibodies

A. (upper panel) Alignement of the two Asf1 isoforms, Asf1a (gi74735206) located on chromosome 6q22, and Asf1b (gi74734533) located on chromosome 19p13, was performed using ClustalW software (http://www.ebi.ac.uk/Tools/clustalw2/). Secondary structures in the conserved N-terminal region (red) are indicated above the sequences. The C-terminus of Asf1a and Asf1b is more variable, harboring potential phosphorylation sites. Amino-acids that differ between Asf1a and Asf1b are in green. Asterisks: identical residues, double dots: conserved residues; single dots: semiconserved substitutions. **(lower panel)** Scheme depicting the pourcentage of homology between the different parts of Asf1a and Asf1b. Specific antibodies against Asf1a were raised against the full GST-Asf1a protein, whereas specific Asf1b antibodies were raised against a GST-C-Term-Asf1b (amino-acids 156 to 202).

B. Western blot analysis of the two Asf1 antibodies on recombinant His-C-Terminal Asf1a and His-C-Terminal Asf1b showing a high specificity of these two antibodies on recombinant proteins. M: molecular weight marker.

C. Western blot analysis of Asf1 antibodies on total extracts from human U-2-OS cells, depleted of Asf1a, Asf1b, or Asf1a+b by siRNA for 48h. Increasing amounts (x) of total cell extracts are loaded and α-tubulin serves as a loading control. While Asf1a antibody #28134 highly recognizes Asf1a and detects a faint band of Asf1b, Asf1b antibody #18143 is highly specific. M: molecular weight marker.

D. Immunofluorescence analysis of U-2-OS cells treated as in (C) underscores the high specificity of the two Asf1 antibodies. DAPI stains nuclei. Scale bar is 20 μm.

Supplementary Figure S2: Asf1a and Asf1b levels across the cell cycle in HeLa cells.

A. Flow cytometry analysis of Hela cells asynchronously growing (AS) or released from a double-thymidine block at the following times : 0h (G1/S), 4h (S), 8h (S/G2), and 14h (G1). Mitotic cells (M) were collected after a 20h nocodazole block.

B. Quantitative RT-PCR analysis of Asf1a and Asf1b mRNA levels across the cell cycle in HeLa cells. Levels are normalized to the reference gene ribosomal protein Po-like protein (RPLPO) (de Cremoux et al, 2004). (a.u.): arbitrary units. Error bars represent data from two independent experiments.

C. Western blot analysis of Asf1a and Asf1b levels in synchronized HeLa cells treated as in (A). Increasing amounts (x) of total cell extracts are loaded and memcode staining (Invitrogen) serves as a loading control. Cyclin A, CAF-1 p60, and PCNA are shown for comparison. M: molecular weight marker.

Supplementary Figure S3: Asf1b levels follows the cycling capacity of cells.

A. Flow cytometry analysis of the cell cycle distribution of asynchronous (AS) or quiescent (G0) U-2-OS cells.

B. Specific expression of Asf1a, Asf1b and the largest subunit of CAF-1 (p150) revealed by immunofluorescence in U-2-OS cells asynchronous (AS) or quiescent (G0). DAPI stains nuclei. Scale bar is 10 μm.

C. Western blot analysis of total MCF7 breast cancer cell extracts from asynchronous (AS), quiescent (G0) or cells released from quiescence for the indicated times (2, 4, 8 and 24 hours). For increasing amounts (x) of total cell extracts, we revealed Asf1a and Asf1b with a mix of the specific Asf1 antibodies. We use α-tubulin as a loading control, CAF-1 p60, PCNA and Cyclin A as markers for cell proliferation. M: molecular weight marker.

D. Asf1a and Asf1b mRNA levels in proliferating (AS), quiescent (G0) and MCF7 cells released from G0 are determined by Quantitative RT-PCR. Levels are normalized as in Figure 1. The error bars represent s.d. from 3 independent experiments.

E. Specific expression of Asf1a, Asf1b and the largest subunit of CAF-1 (p150) revealed by immunofluorescence in MCF7 cells asynchronous (AS), quiescent (G0), or released from G0 for the indicated times. DAPI stains nuclei. Scale bar is 20 μm.

F. Flow cytometry analysis of the cell cycle distribution of the cells shown in C.

Supplementary Figure S4: Validation of transcriptomic data.

A. Quantitative RT-PCR analysis of Asf1a and Asf1b mRNA levels in U-2-OS cells depleted for Asf1a, Asf1b or Asf1(a+b) for 48h by siRNA treatment. mRNA levels are normalized to the reference gene GAPDH and expressed as the log2(fold change) relative to the control siRNA. The error bar represents data from three independent experiments.

B. Quantitative RT-PCR analysis of mRNA levels for the indicated genes in U-2-OS cells treated as in (A). mRNA levels are normalized as in (A). The error bar represents data from three independent experiments respectively. Below each graph is indicated the numerical value for the mean log2 fold change (FC) obtained on the Affymetrix microarray (2 independent experiments). (See Supplementary Figure S9A-B for the specific depletion and

cell cycle profiles of U-2-OS cells depleted of Asf1 isoforms with two independent sets of siRNAs).

C. Clustering analysis of all differentially expressed genes ($p<0.05$). Relative up (Blue) or down (Red) expression of a given gene is compared to the mean value of that gene in all samples. For each gene, the mean value is set to 0 and the variance to 1. This heat map allows visualisation of different groups of genes according to their similar expression values.

Supplementary Figure S5: Asf1b depletion impairs proliferation in U-2-OS cells.

A. Immunofluorescence analysis of human U-2-OS cells showing the specific depletion of Asf1a, Asf1b or Asf1(a+b) for 48h by RNA interference with two independent sets of siRNAs. DAPI stains nuclei. Scale bar is 10 mm.

B. Histograms show quantitative analysis of the proportion of aberrant nuclear structures in U-2-OS cells treated as in (A). The mean percentage of altered nuclei (lobulated) and the percentage of micronucleated cells after 48h of siRNA treatment are plotted. Errors bars represent data from three and two independent experiments, respectively. Surprisingly, the combined depletion of Asf1(a+b) did not give as strong an effect as Asf1b depletion alone on nuclei morphology. It is possible that the slow S phase progression observed in the double Asf1 knockdown may potentially prevent the detection of defects observed after depletion of Asf1b alone for 48 hours.

C. Immunofluorescence analysis of Lamin A staining in U-2-OS cells treated as in (A). DAPI stains nuclei. Scale bar is 10 μm.

D. Colony Formation Assay for U-2-OS cells treated with two independent sets of siRNAs against Asf1 isoforms. The mean surviving fraction (%) is indicated in the histogramms. Error bars represent data from 2 independent experiments.

Supplementary Figure S6: Specific depletion of Asf1 isoforms in Hs578T cells.

A. Western blot analysis of total extracts from human Hs578T cells showing the specific depletion of Asf1a, Asf1b or Asf1(a+b) for 48h by siRNA treatment with two independent sets of oligonucleotides. Increasing amounts (x) of total cell extracts are loaded. α-tubulin serve as a loading control. We reveal Asf1a and Asf1b with a mix of the specific Asf1 antibodies. M: molecular weight marker.

B. Flow cytometry analysis of the cell cycle distribution of the cells shown in (A). Asf1b depletion slightly increases the number of cells in S/G2 phases. Asf1(a+b) depletion impairs S phase progression as demonstrated previously in U-2-OS cells (Groth et al, 2007).

C. Quantitative RT-PCR analysis of Asf1a and Asf1b mRNA levels in Hs578T cells treated as in (A). mRNA levels are normalized to the reference gene GAPDH and expressed as the log2(fold change) relative to the control siRNA. The error bar represents data from two independent experiments.

Supplementary Figure S7: Depletion of Asf1 isoforms in MDA-MB-231 cells impairs proliferation.

A. Western blot analysis of total extracts from human MDA-MB-231 cells showing the specific depletion of Asf1a, Asf1b or Asf1(a+b) for 48h by siRNA treatment. Increasing amounts (x) of total cell extracts are loaded. α-tubulin serve as a loading control. We reveal Asf1a and Asf1b with a mix of the specific Asf1 antibodies. M: molecular weight marker.

B. Flow cytometry analysis of the cell cycle distribution of the cells shown in (A).

C. (left panel) Immunofluorescence analysis of human MDA-MB-231 cells treated as in (A). Arrowheads marks DNA bridges with micronuclei between cells. DAPI stains nuclei. Scale bar is 10 μm. **(right panel)** Histograms show quantitative analysis of the proportion of aberrant nuclear structures in MDA-MB-231 cells treated as in (A). The mean percentage of altered nuclei (lobulated) and the percentage of DNA bridges after 48h of siRNA treatment are plotted. Errors bars represent data from two independent experiments.

D. Colony Formation Assay for MDA-MB-231 cells treated with one set of siRNAs against Asf1 isoforms as in (A). The mean surviving fraction (%) is indicated in the histogramms. Error bars represent data from 2 independent experiments.

Supplementary Figure S8: Asf1b, a proliferation marker with prognostic value in small breast cancers.

A. Correlations between the logarithmic mRNA expression levels of the indicated genes are depicted. The Pearson coefficient of correlation (r) and its associated p-value are indicated. Red numbers together with an asterisk * indicates a significant p-value ($p<0.05$).

B. Table describing the samples from patients of 1996 with small breast tumors.

C. Univariate Kaplan-Meier curves of the metastasis free interval (interval before the occurrence of metastasis), and the disease free interval (interval before the occurence of local recurrence, regional lymph node recurrence, controlateral breast cancer or metastasis) in patients of 1996 with breast cancer classified as non-palpable (T0) or small (T1-T2), lymph node negative (N0) and metastasis free (M0) and expressing low (Asf1b <0.30) or high

(Asf1>=0.30) levels of Asf1b. Red color indicates a significant p-value ($p<0.05$). The number of patients at risk at each time point is indicated below each graphic.

Supplementary Figure S9: Impact of the specific depletion of Asf1 isoforms at the cellular level.

A. Western blot analysis of total extracts from human U-2-OS cells showing the specific depletion of Asf1a, Asf1b or Asf1(a+b) for 48h by siRNA treatment with two independent sets of oligonucleotides. Increasing amounts (x) of total cell extracts are loaded. α-tubulin and Memcode serve as a loading control. We reveal Asf1a and Asf1b with a mix of the specific Asf1 antibodies and we reveal γH2A.X. M: molecular weight marker.

B. Flow cytometry analysis of the cell cycle distribution of the cells shown in (A). Neither Asf1a nor Asf1b depletions give any obvious phenotype during S phase. The upregulation of Asf1a in cells depleted of Asf1b (Figure 3B) could represent a compensatory mechanism to allow normal S phase progression.

C. (Left panel) Immunofluorescence analysis of PCNA staining in U-2-OS cells treated as in (A). Representive mid S phase patterns are shown. DAPI stains nuclei. Scale bar is 10 μm. **(Right panel)** Quantification of the mean number of PCNA positive cells at 48h in cells treated as in (A). The percentage of early, mid and late S phase patterns are calculated among the PCNA positive cells. Error bars represent data from 2 independent experiments respectively.

D. (Left panel) Western Blot analysis of total extracts from human U-2-OS cells treated with the indicated siRNAs for 96h. α-tubulin and Memcode serve as a loading control. We reveal Asf1a and Asf1b with a mix of the specific Asf1 antibodies and we reveal γH2A.X. M: molecular weight marker. **(Right panel)** Western Blot analysis of total extracts from human HeLa cells treated with the indicated siRNAs for 72h performed as above. We hypothesize that Asf1a alone is not sufficient to replace the function of Asf1b during replication. This insufficient role of Asf1a in the absence of Asf1b could lead to an impaired chromatin assembly during S-phase, leading to accumulation of damage.

Supplementary Figure S10: Asf1b correlates with prognosis in breast cancer and is overexpressed in multiple types of cancer.

A. Boxplot representation of microarray expression levels of Asf1b in relation to prognosis in different breast cancer transcriptomes, including some validation studies of the Mammaprint

prognostic signature (Desmedt et al, 2007; Sorlie et al, 2001; van de Vijver et al, 2002). Asf1b expression levels significantly correlate with the grade of the tumor (left), with the occurence of metastasis at 5 years (middle) and with the disease free survival at 5 years (right). Results are analyzed and plotted using ONCOMINE database (Rhodes et al, 2004). Boxes represent the 25th-75th percentile, brackets: range; black line: median; black dots: outliers; n: sample number. We considered p-values, based on Student's T-test, as significant when $p \leq 0.05$.

B. Boxplot representation as in (A) of microarray expression levels of Asf1b in different types of cancer (red) compared to normal tissue (blue). Results from transcriptome studies on different tumor types (Chen et al, 2002; Hendrix et al, 2006; Richardson et al, 2006; Su et al, 2007; Talantov et al, 2005) are analyzed and plotted using ONCOMINE database (Rhodes et al, 2004)**.** We considered p-values, based on Student's T-test, as significant when $p \leq 0.05$.

Supplementary Table SI: List of all primary antibodies used in this study.

Company, as well as the order number, the lot number, the species and the dilutions for western blotting (WB) and immunofluorescence (IF) are provided for each antibody. Since Asf1a and Asf1b migrate at different positions in western blot (Sillje & Nigg, 2001), we used a mix of the specific Asf1 antibodies in western blot to recognize simultaneously the two isoforms. The specific purified antibodies against Asf1a or Asf1b were used separately in immunofluorescence.

Supplementary Table SII:

A. Table describing the samples from patients of 1995 with small breast tumors.

B. Comparison of Asf1a, Asf1b, CAF-1 p60, CAF-1 p150 and Ki67 between multiple groups of prognostic factors in the set of tumor samples from 1995. (Upper part) Correlations between the indicated genes and clinicopathological factors. N: number of samples included in the statistical analysis for each gene. Significant p-values (≤ 0.05) are noted in bold. (Lower part) Correlations between the genes. r: Pearson coefficient of correlation. Significant p-values (≤ 0.05) are noted in bold.

Supplementary Table SIII. Multivariate analysis in patients of 1996.

Multivariate analysis adjusted for known prognostic factors (such as mitotic index, tumor size, tumor grade and Ki67 levels) and for our genes of interest (Asf1b, CAF-1 p60, CAF-1

p150 and HP1α when significant in univariate analysis) in n=62 samples. This analysis performed on an independent set of patients confirms the prognostic value of Asf1b in predicting metastasis occurence. In each case, the significant p-value ($p<0.05$), the Relative Risk (RR) and the 95% Confidence Interval (CI) are indicated.

Supplementary References

Alexa A, Rahnenfuhrer J, Lengauer T (2006) Improved scoring of functional groups from gene expression data by decorrelating GO graph structure. *Bioinformatics* **22**(13)**:** 1600-1607

Ashburner M, Ball CA, Blake JA, Botstein D, Butler H, Cherry JM, Davis AP, Dolinski K, Dwight SS, Eppig JT, Harris MA, Hill DP, Issel-Tarver L, Kasarskis A, Lewis S, Matese JC, Richardson JE, Ringwald M, Rubin GM, Sherlock G (2000) Gene ontology: tool for the unification of biology. The Gene Ontology Consortium. *Nat Genet* **25**(1)**:** 25-29

Benjamini Y, Drai D, Elmer G, Kafkafi N, Golani I (2001) Controlling the false discovery rate in behavior genetics research. *Behav Brain Res* **125**(1-2)**:** 279-284

Birney E, Andrews TD, Bevan P, Caccamo M, Chen Y, Clarke L, Coates G, Cuff J, Curwen V, Cutts T, Down T, Eyras E, Fernandez-Suarez XM, Gane P, Gibbins B, Gilbert J, Hammond M, Hotz HR, Iyer V, Jekosch K, Kahari A, Kasprzyk A, Keefe D, Keenan S, Lehvaslaiho H, McVicker G, Melsopp C, Meidl P, Mongin E, Pettett R, Potter S, Proctor G, Rae M, Searle S, Slater G, Smedley D, Smith J, Spooner W, Stabenau A, Stalker J, Storey R, Ureta-Vidal A, Woodwark KC, Cameron G, Durbin R, Cox A, Hubbard T, Clamp M (2004) An overview of Ensembl. *Genome Res* **14**(5)**:** 925-928

Carroll JS, Prall OW, Musgrove EA, Sutherland RL (2000) A pure estrogen antagonist inhibits cyclin E-Cdk2 activity in MCF-7 breast cancer cells and induces accumulation of p130-E2F4 complexes characteristic of quiescence. *J Biol Chem* **275**(49)**:** 38221-38229

Chen X, Cheung ST, So S, Fan ST, Barry C, Higgins J, Lai KM, Ji J, Dudoit S, Ng IO, Van De Rijn M, Botstein D, Brown PO (2002) Gene expression patterns in human liver cancers. *Mol Biol Cell* **13**(6)**:** 1929-1939

Dai M, Wang P, Boyd AD, Kostov G, Athey B, Jones EG, Bunney WE, Myers RM, Speed TP, Akil H, Watson SJ, Meng F (2005) Evolving gene/transcript definitions significantly alter the interpretation of GeneChip data. *Nucleic Acids Res* **33**(20)**:** e175

de Cremoux P, Bieche I, Tran-Perennou C, Vignaud S, Boudou E, Asselain B, Lidereau R, Magdelenat H, Becette V, Sigal-Zafrani B, Spyratos F (2004) Inter-laboratory quality control for hormone-dependent gene expression in human breast tumors using real-time reverse transcription-polymerase chain reaction. *Endocr Relat Cancer* **11**(3)**:** 489-495

Desmedt C, Piette F, Loi S, Wang Y, Lallemand F, Haibe-Kains B, Viale G, Delorenzi M, Zhang Y, d'Assignies MS, Bergh J, Lidereau R, Ellis P, Harris AL, Klijn JG, Foekens JA, Cardoso F, Piccart MJ, Buyse M, Sotiriou C (2007) Strong time dependence of the 76-gene prognostic signature for node-negative breast cancer patients in the TRANSBIG multicenter independent validation series. *Clin Cancer Res* **13**(11)**:** 3207-3214

Gentleman RC, Carey VJ, Bates DM, Bolstad B, Dettling M, Dudoit S, Ellis B, Gautier L, Ge Y, Gentry J, Hornik K, Hothorn T, Huber W, Iacus S, Irizarry R, Leisch F, Li C, Maechler M, Rossini AJ, Sawitzki G, Smith C, Smyth G, Tierney L, Yang JY, Zhang J (2004) Bioconductor: open software development for computational biology and bioinformatics. *Genome Biol* **5**(10)**:** R80

Groth A, Corpet A, Cook AJ, Roche D, Bartek J, Lukas J, Almouzni G (2007) Regulation of replication fork progression through histone supply and demand. *Science* **318**(5858)**:** 1928-1931

Hendrix ND, Wu R, Kuick R, Schwartz DR, Fearon ER, Cho KR (2006) Fibroblast growth factor 9 has oncogenic activity and is a downstream target of Wnt signaling in ovarian endometrioid adenocarcinomas. *Cancer Res* **66**(3)**:** 1354-1362

Huber W, von Heydebreck A, Sultmann H, Poustka A, Vingron M (2002) Variance stabilization applied to microarray data calibration and to the quantification of differential expression. *Bioinformatics* **18 Suppl 1:** S96-104

Kauffmann A, Gentleman R, Huber W (2009) arrayQualityMetrics--a bioconductor package for quality assessment of microarray data. *Bioinformatics* **25**(3)**:** 415-416

Martini E, Roche DM, Marheineke K, Verreault A, Almouzni G (1998) Recruitment of phosphorylated chromatin assembly factor 1 to chromatin after UV irradiation of human cells. *J Cell Biol* **143**(3)**:** 563-575

Mello JA, Sillje HH, Roche DM, Kirschner DB, Nigg EA, Almouzni G (2002) Human Asf1 and CAF-1 interact and synergize in a repair-coupled nucleosome assembly pathway. *EMBO Rep* **3**(4)**:** 329-334

Moggs JG, Grandi P, Quivy JP, Jonsson ZO, Hubscher U, Becker PB, Almouzni G (2000) A CAF-1-PCNA-mediated chromatin assembly pathway triggered by sensing DNA damage. *Mol Cell Biol* **20**(4)**:** 1206-1218

Rhodes DR, Yu J, Shanker K, Deshpande N, Varambally R, Ghosh D, Barrette T, Pandey A, Chinnaiyan AM (2004) ONCOMINE: a cancer microarray database and integrated data-mining platform. *Neoplasia* **6**(1)**:** 1-6

Richardson AL, Wang ZC, De Nicolo A, Lu X, Brown M, Miron A, Liao X, Iglehart JD, Livingston DM, Ganesan S (2006) X chromosomal abnormalities in basal-like human breast cancer. *Cancer Cell* **9**(2)**:** 121-132

Sillje HH, Nigg EA (2001) Identification of human Asf1 chromatin assembly factors as substrates of Tousled-like kinases. *Curr Biol* **11**(13)**:** 1068-1073

Smyth GK (2004) Linear models and empirical bayes methods for assessing differential expression in microarray experiments. *Stat Appl Genet Mol Biol* **3:** Article3

Sorlie T, Perou CM, Tibshirani R, Aas T, Geisler S, Johnsen H, Hastie T, Eisen MB, van de Rijn M, Jeffrey SS, Thorsen T, Quist H, Matese JC, Brown PO, Botstein D, Eystein Lonning P, Borresen-Dale AL (2001) Gene expression patterns of breast carcinomas distinguish tumor subclasses with clinical implications. *Proc Natl Acad Sci U S A* **98**(19)**:** 10869-10874

Su LJ, Chang CW, Wu YC, Chen KC, Lin CJ, Liang SC, Lin CH, Whang-Peng J, Hsu SL, Chen CH, Huang CY (2007) Selection of DDX5 as a novel internal control for Q-RT-PCR from microarray data using a block bootstrap re-sampling scheme. *BMC Genomics* **8:** 140

Talantov D, Mazumder A, Yu JX, Briggs T, Jiang Y, Backus J, Atkins D, Wang Y (2005) Novel genes associated with malignant melanoma but not benign melanocytic lesions. *Clin Cancer Res* **11**(20)**:** 7234-7242

van de Vijver MJ, He YD, van't Veer LJ, Dai H, Hart AA, Voskuil DW, Schreiber GJ, Peterse JL, Roberts C, Marton MJ, Parrish M, Atsma D, Witteveen A, Glas A, Delahaye L, van der Velde T, Bartelink H, Rodenhuis S, Rutgers ET, Friend SH, Bernards R (2002) A gene-expression signature as a predictor of survival in breast cancer. *N Engl J Med* **347**(25)**:** 1999-2009

Supplementary Figure S1

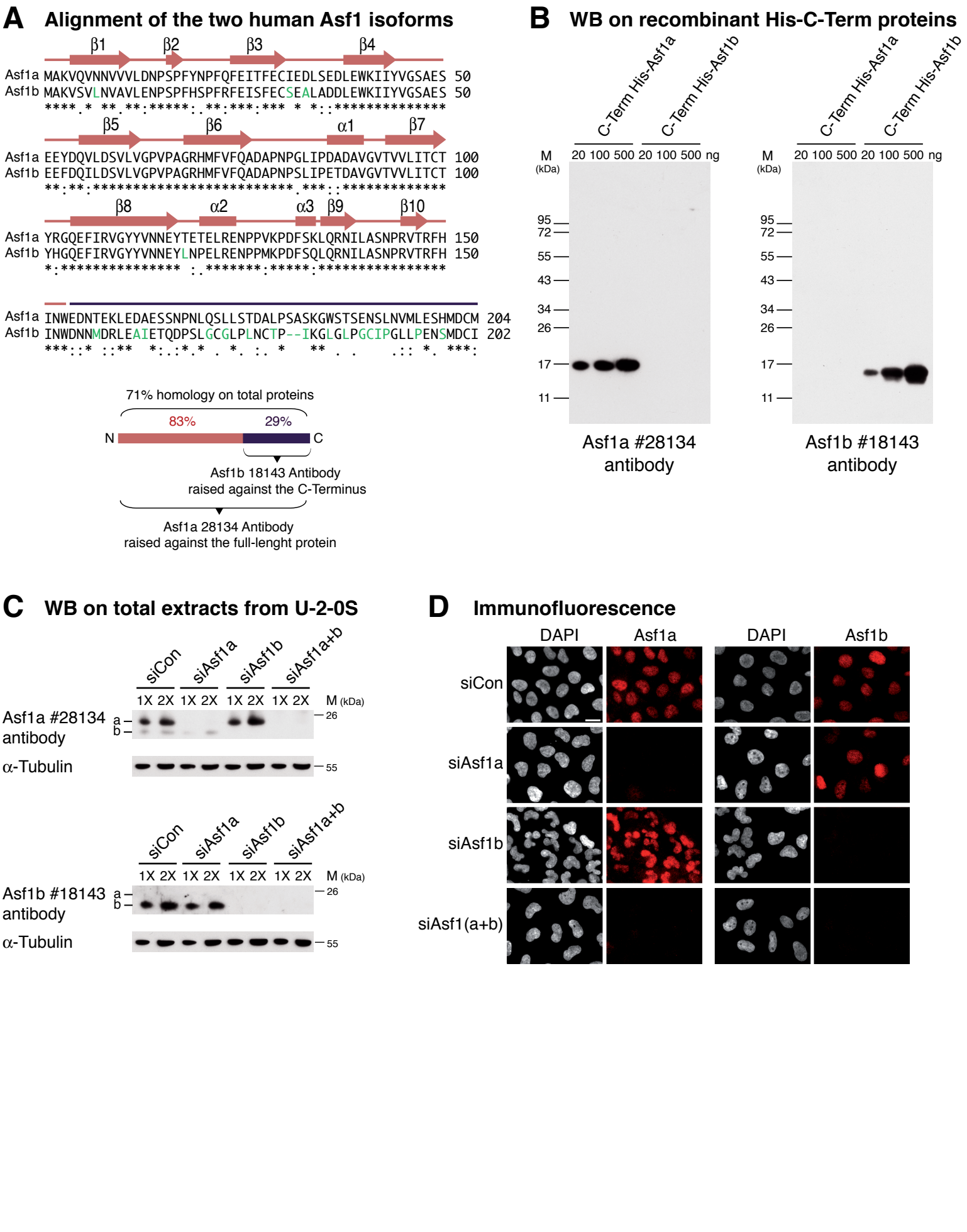

Supplementary Figure S2

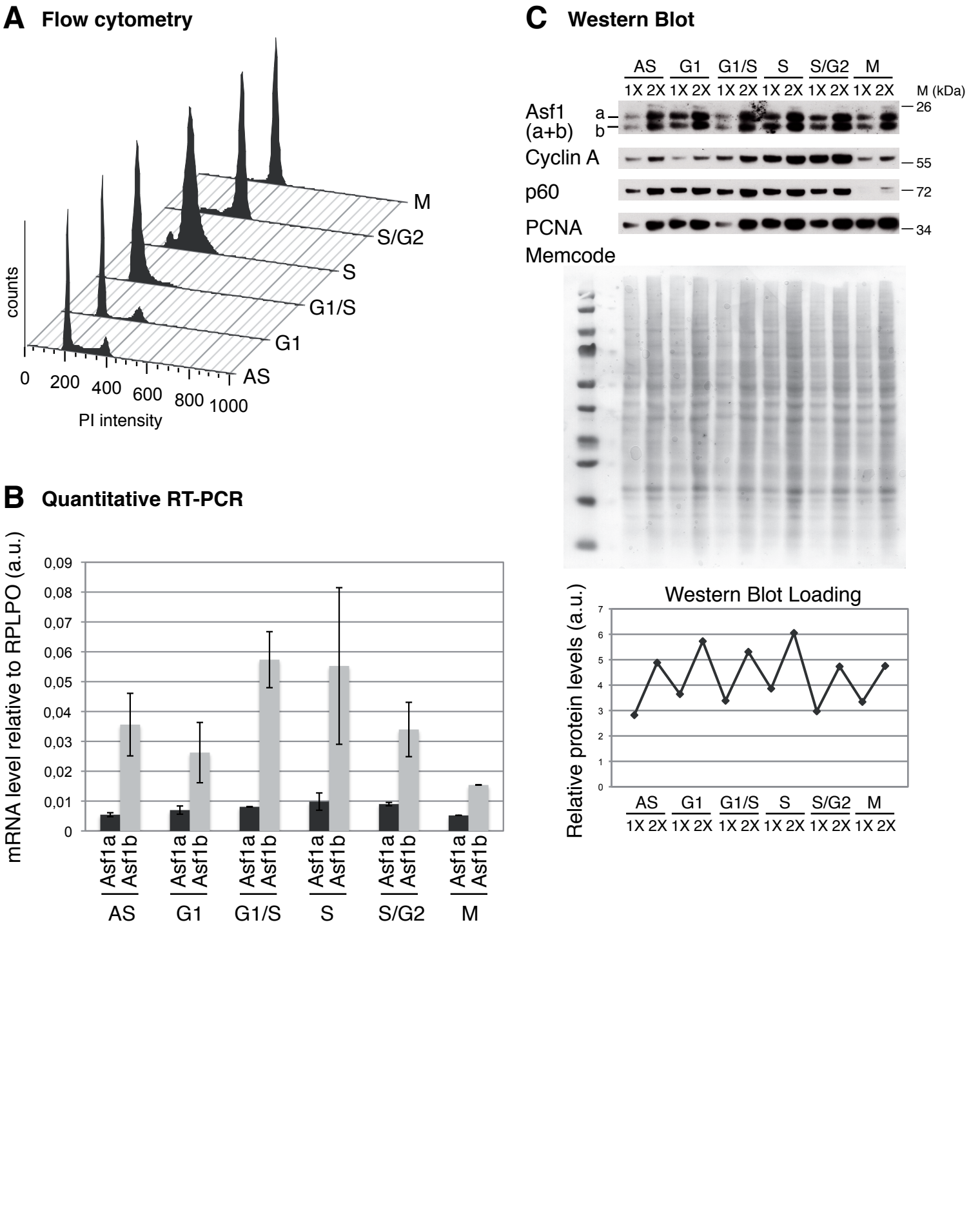

Supplementary Figure S3

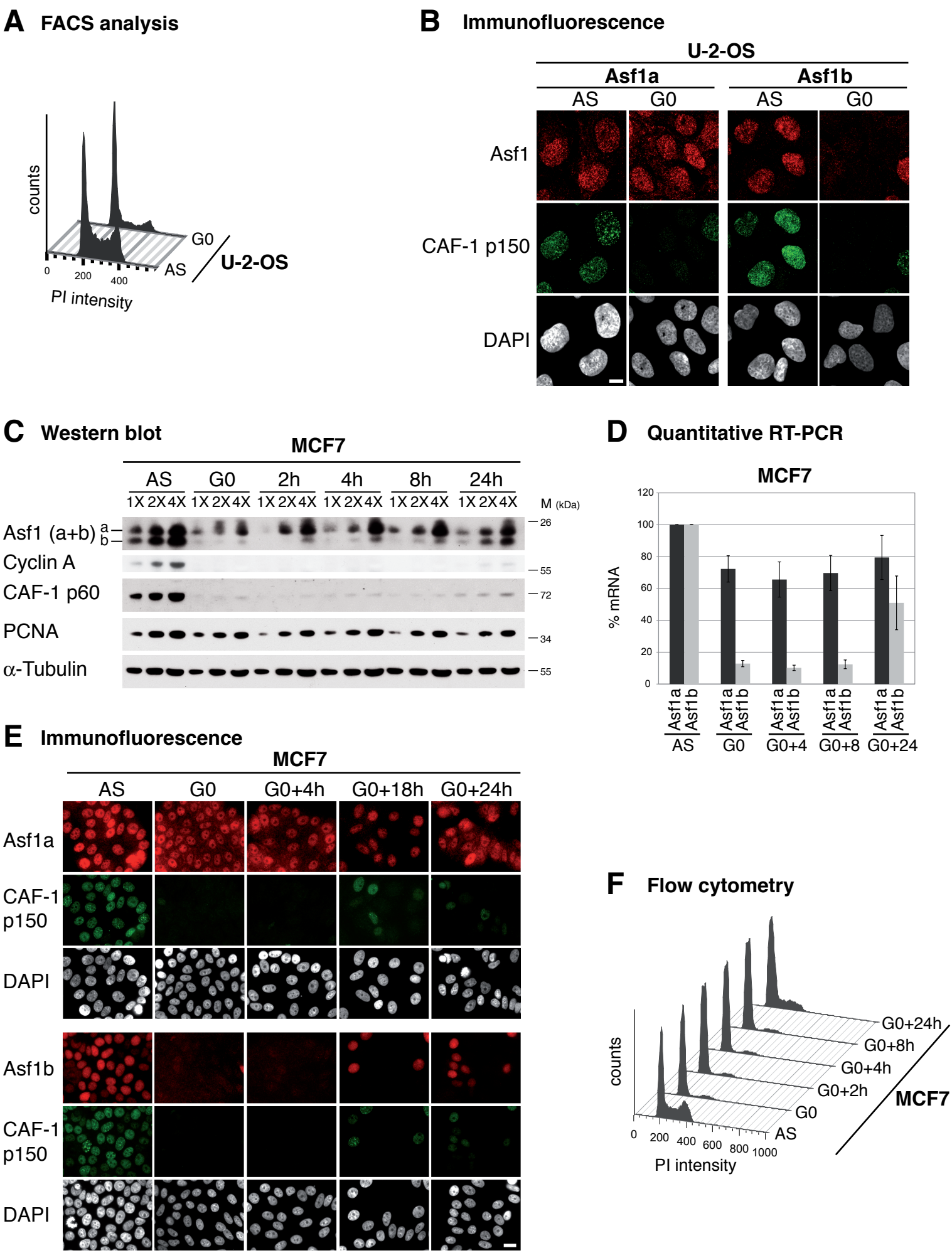

Supplementary Figure S4

A Validation of Asf1a and Asf1b depletions by Q-RT-PCR

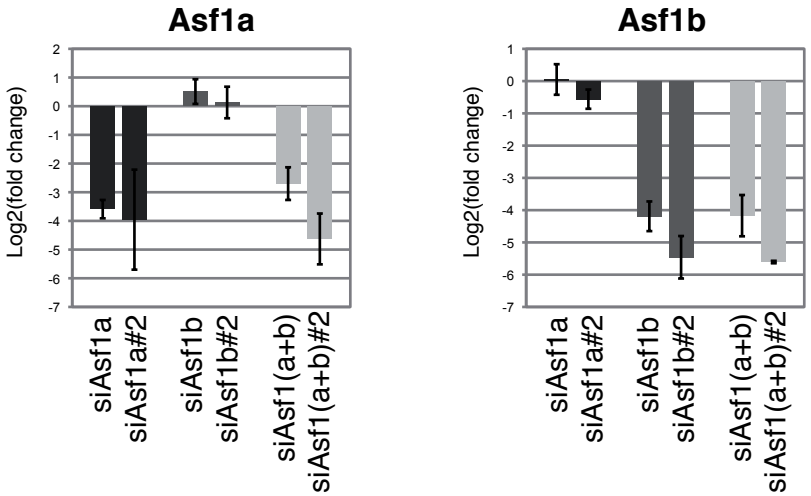

B Validation of differentially expressed genes by Q-RT-PCR

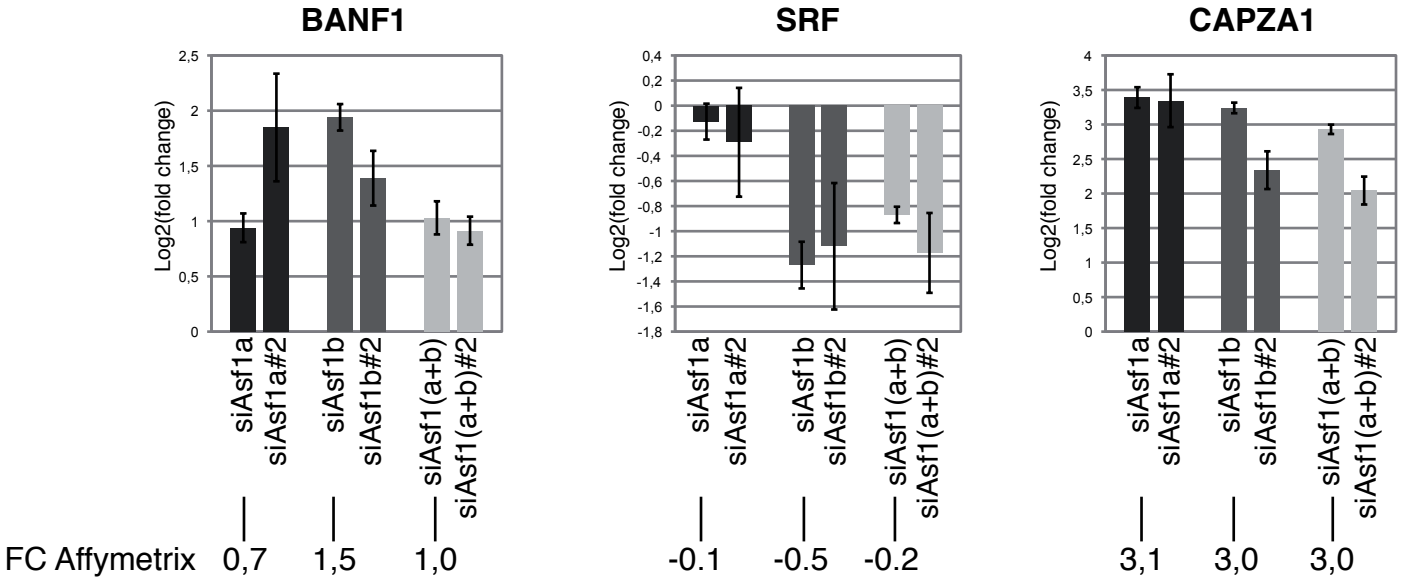

C Heatmap of differentially expressed genes (p<0.05)

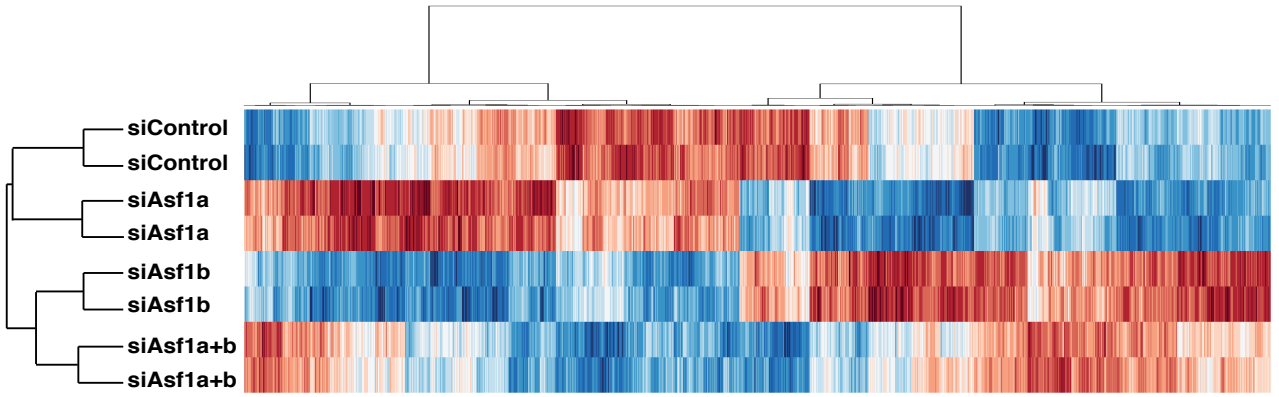

Supplementary Figure S5:
Depletion of Asf1 in U-2-OS cells impairs proliferation

A **Cellular defects upon specific depletion of Asf1 isoforms**

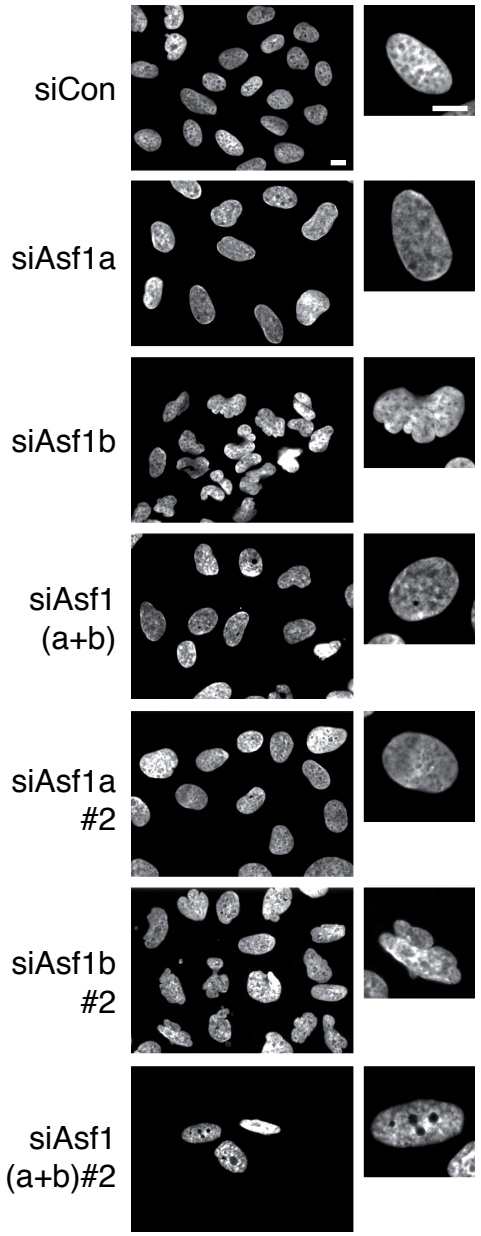

B **Aberrant structures quantification**

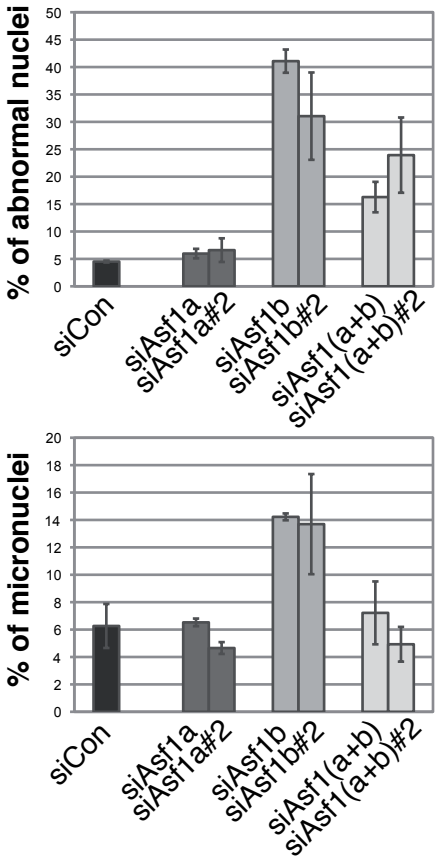

C **Immunofluorescence in U-2-OS cells**

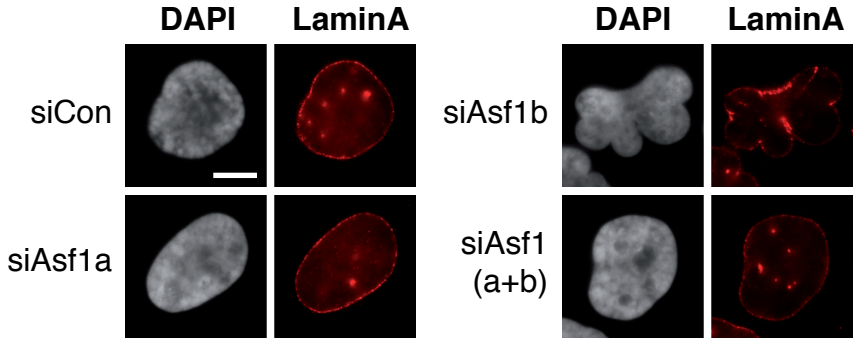

D **Colony formation assay upon specific depletion of Asf1 isoforms in U-2-OS cells**

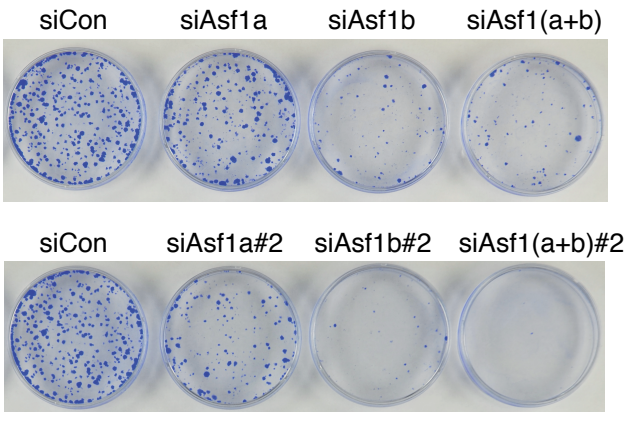

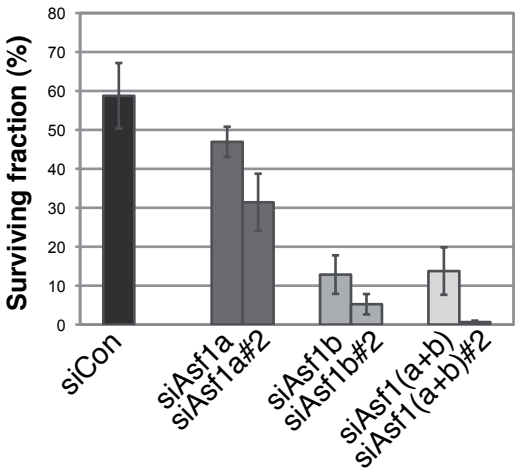

Supplementary Figure S6
Specific depletion of Asf1 isoforms in Hs578T cells

A **Western Blot**

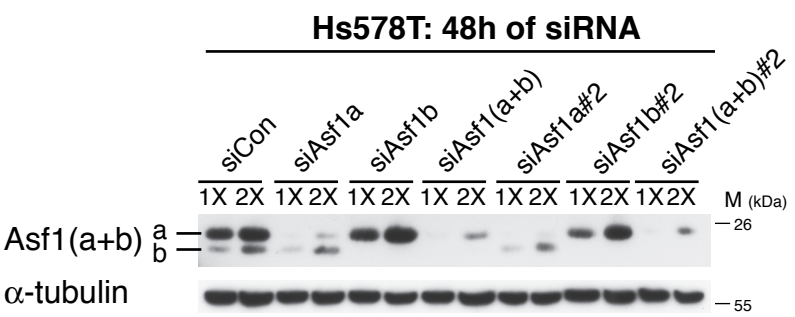

B **FACS**

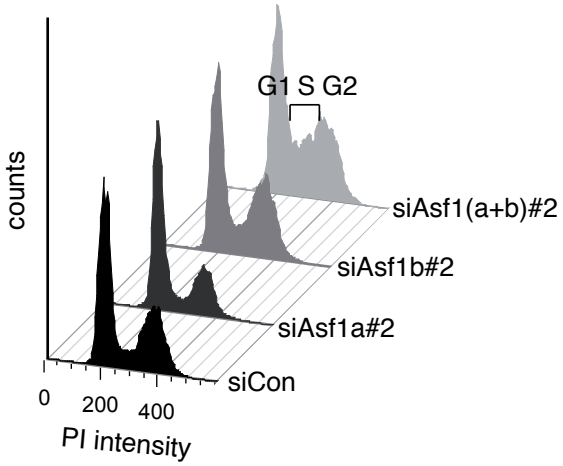

C **Q-RT-PCR**

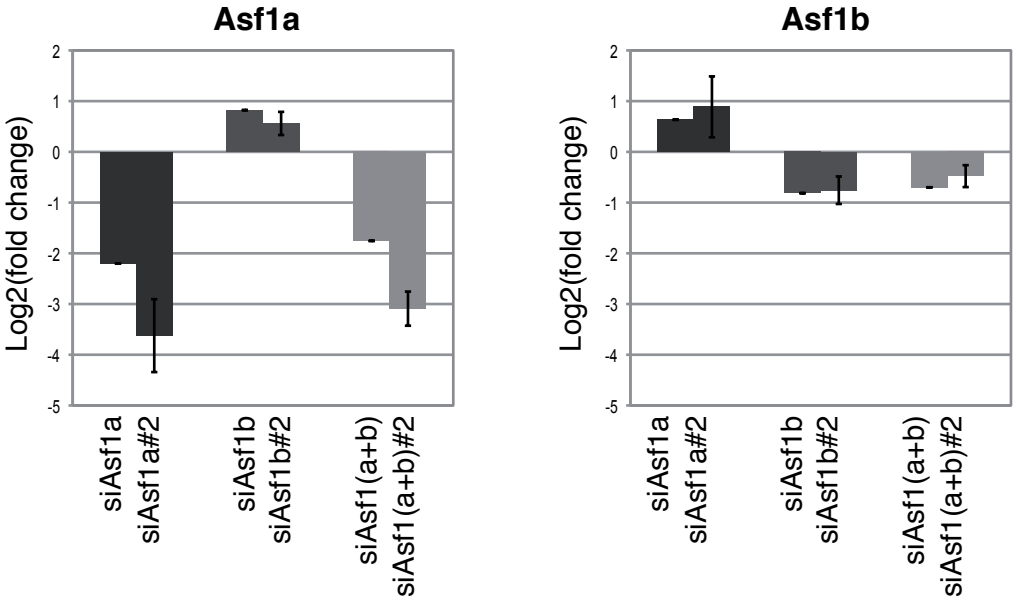

Supplementary Figure S7
Depletion of Asf1 isoforms in MDA-MB-231 cells impairs proliferation

A Specific depletion of Asf1 isoforms

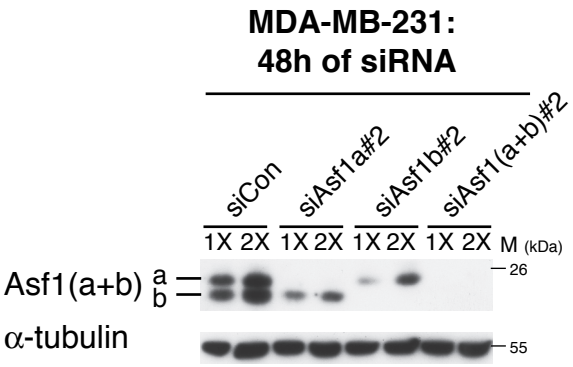

B FACS

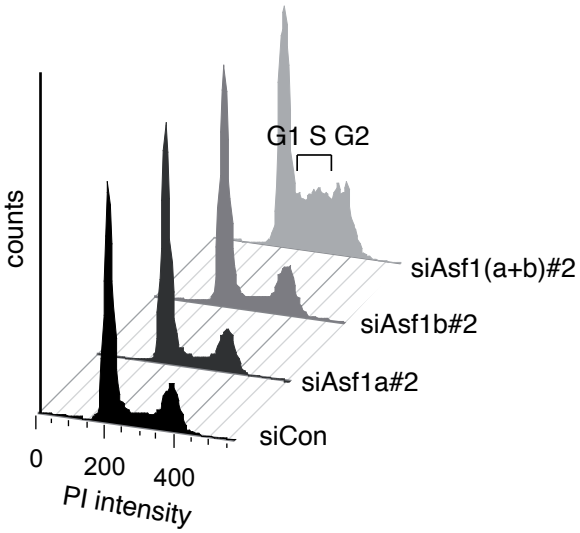

C Cellular defects upon specific depletion of Asf1 isoforms in MDA-MB-231 cells

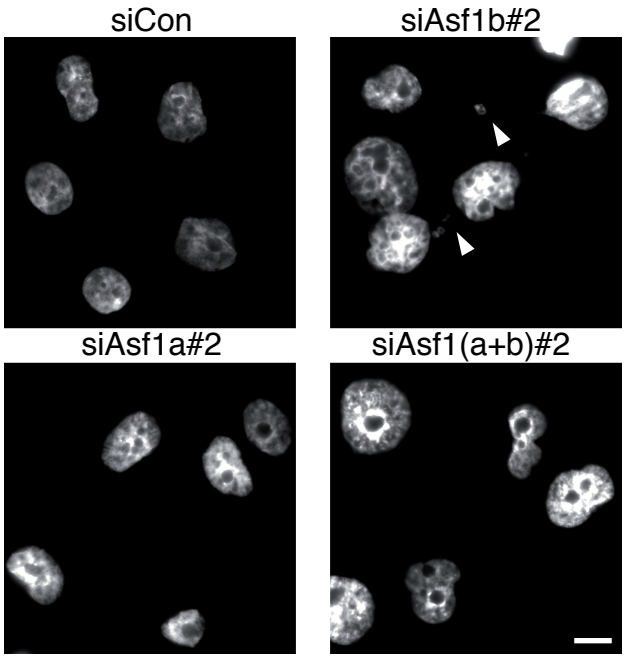

Aberrant structures quantification

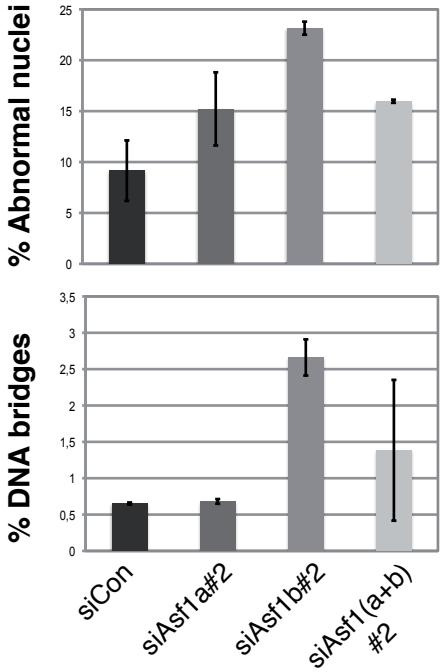

D Colony formation assay upon specific depletion of Asf1 isoforms in MDA-MB-231 cells

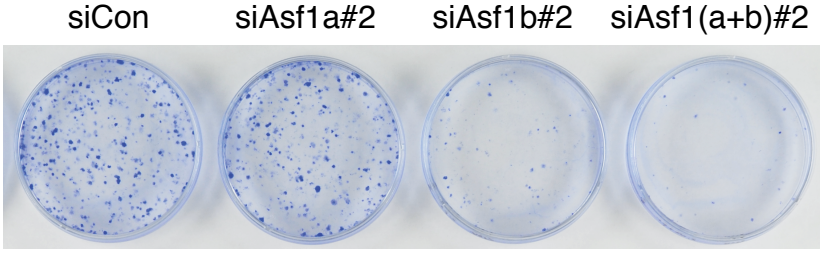

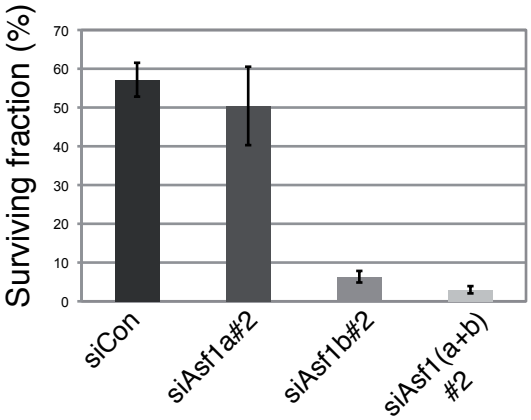

Supplementary Figure S8

A Correlations between genes

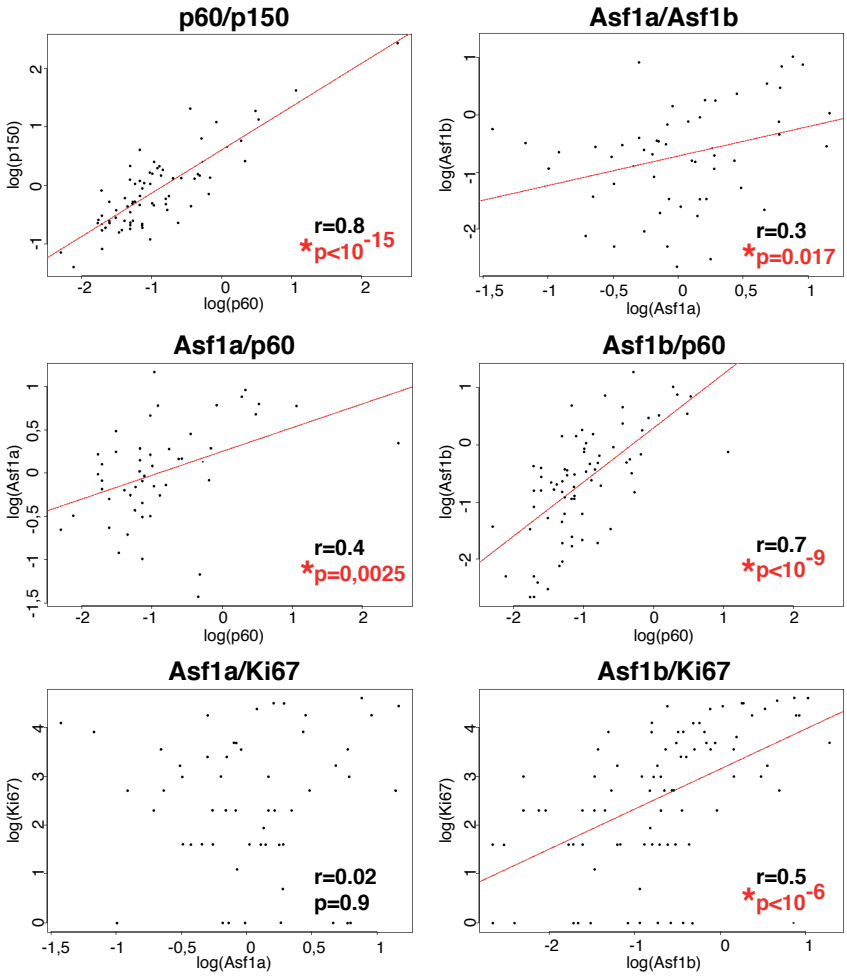

B Description of the samples from patients of 1996 with small breast tumors

Age	Median: 55 (range: 30-69)		**Size classification**	T0/T1	66%	**ER**	(+) 80% / (-) 20%	
Menopaused	Yes	37%		T2	34%	**PR**	(+) 77% / (-) 23%	
	No	63%	**Tumor size (mm)**	Median: 20 (range: 8-35)		**Ki67**	<= 15	44%
Histological type	ductal	74%	**Mitotic index**	Median: 5 (range: 0-120)			15-40	25%
	lobular	16%	**Grade EE**	I	30%		> 40	31%
	tubular	1%		II	48%	**Adjuvant chemotherapy**	No	93%
	other	9%		III	22%		Yes	7%

C Prognostic value of Asf1b in (T0/T1/T2-N0-M0) breast cancers from 1996

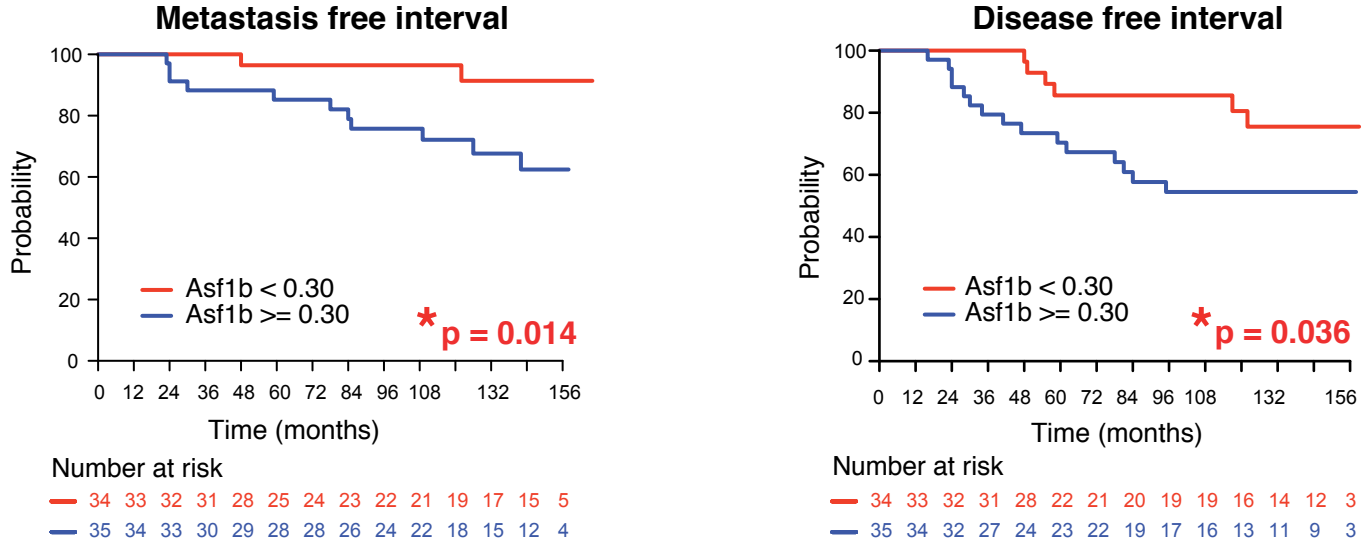

Supplementary Figure S9

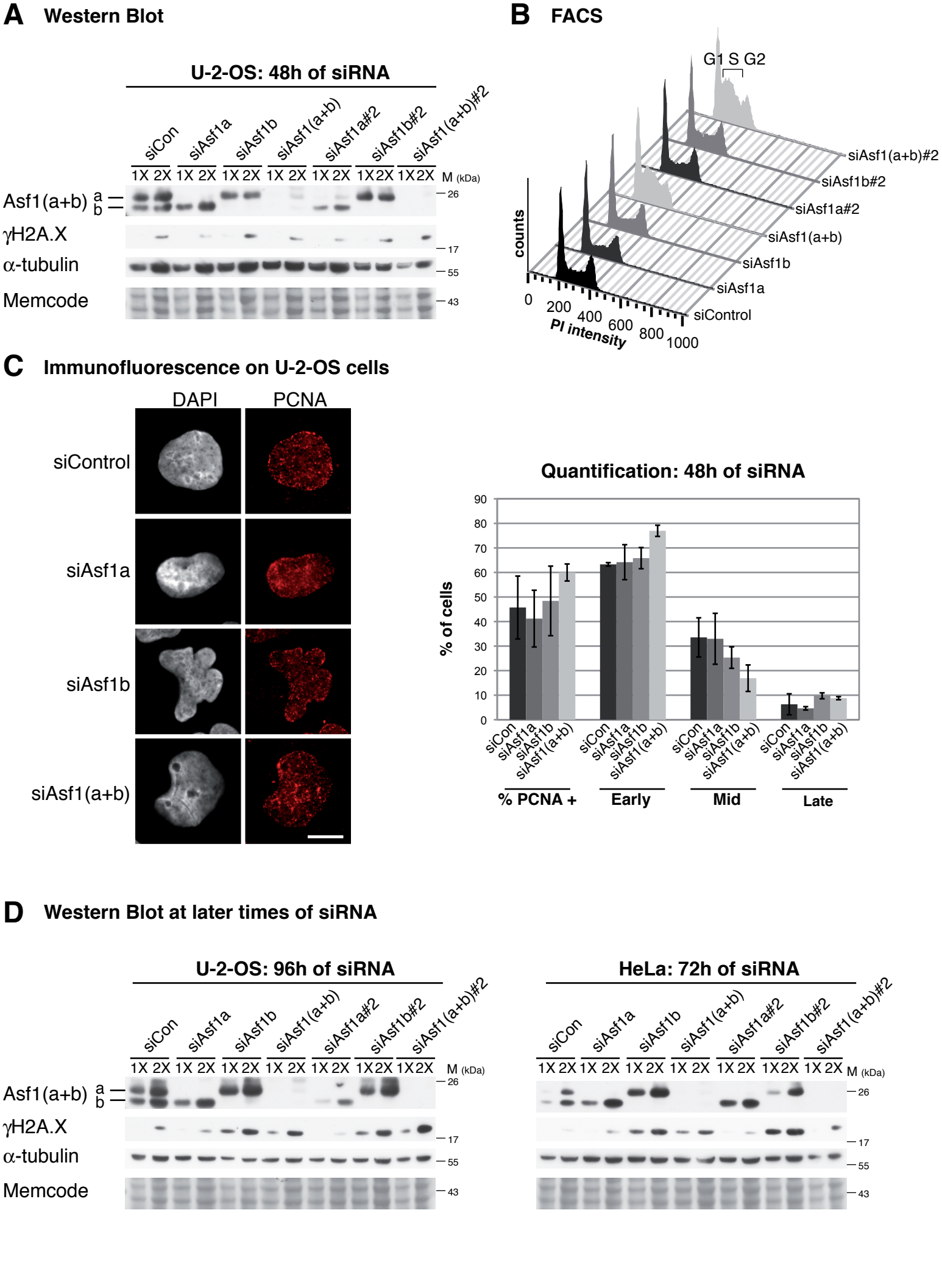

Supplementary Figure S10

A Prognosis value in Breast cancer

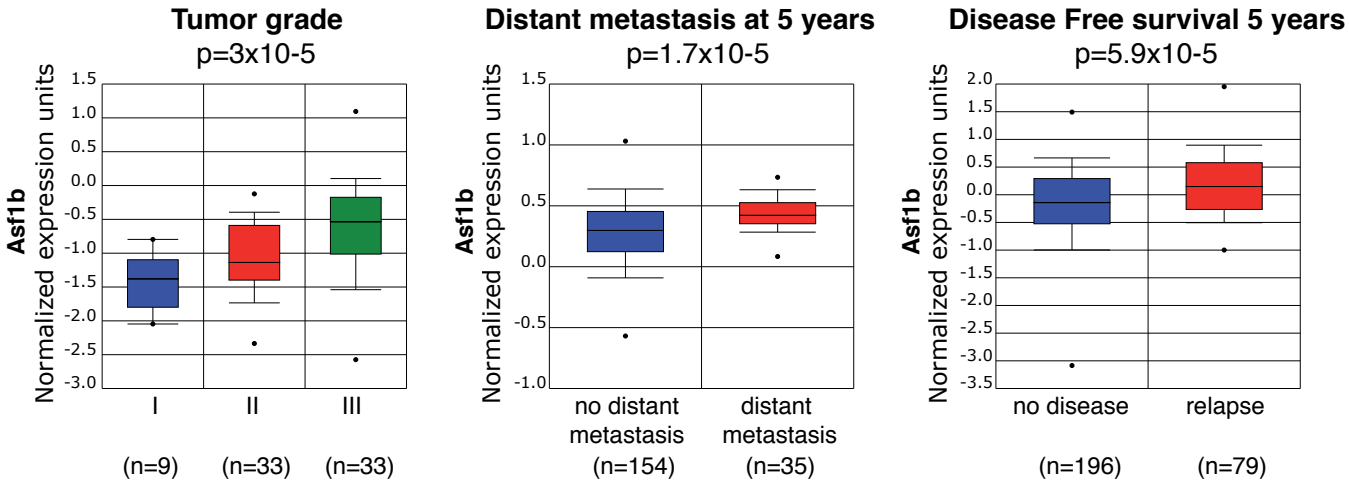

B Tumoral versus normal microarray expression data

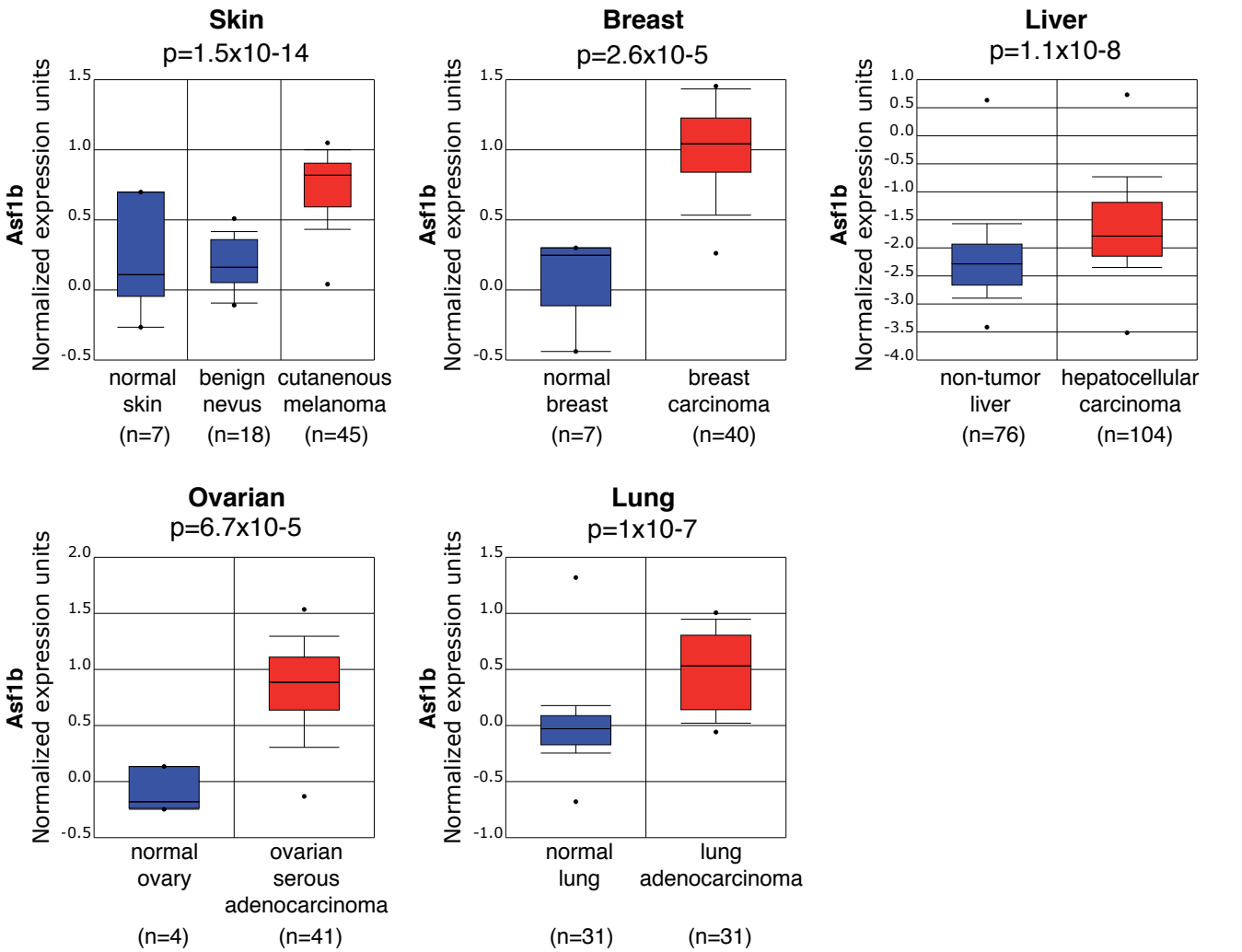

Supplementary Table SI

Antibody	Company/Reference	Order Number	Lot number	Species	WB dilution	IF dilution
Asf1a	Mello et al., 2002	———	#28134	Rabbit polyclonal	mix (a+b) 1/1000 each	1/2000 purified
Asf1b	This study	———	#18143	Rabbit polyclonal		1/500 purified
α-Tubulin	Sigma	T9026 (DM1A)	104K4800	Mouse monoclonal	1/10 000	———
CAF-1 p60	Quivy et al., 2008	———	#17019	Rabbit polyclonal	1/1000	———
CAF-1 p150	Abcam	ab7655	588276	Mouse monoclonal	———	1/1000
CyclinA	Santa Cruz	sc-751	G0104	Rabbit polyclonal	1/1000	———
LaminA/C	Cell signaling	2032	2	Rabbit polyclonal	———	1/50
PCNA	DAKO	M0879 (PC-10)	00026418	Mouse monoclonal	1/2000	———
Phospho-H2A.X (Ser139)	Millipore	05-636	DAM1567248	Mouse monoclonal	1/1000	———

Supplementary Table SII

A Description of the samples from patients of 1995 with small breast tumors

Age	Median: 53 (range: 26-70)		**Size classification**	T0/T1	62%	**ER**	(+) 86% / (-) 14%	
Menopaused	Yes	54%		T2	38%	**PR**	(+) 69% / (-) 31%	
	No	46%	**Tumor size (mm)**	Median: 18 (range: 6-50)		**Ki67**	<= 15	52%
Histological type	ductal	88%	**Mitotic index**	Median: 8 (range: 0-105)			15-40	24%
	lobular	9%	**Grade EE**	I	33%		> 40	24%
	papillary	1%		II	42%	**Adjuvant chemotherapy**	No	93%
	tubular	1%		III	25%		Yes	7%

B Comparison of Asf1a, Asf1b, CAF-1 p60, CAF-1 p150 and Ki67 between multiple groups of prognostic factors in samples from 1995

	Asf1a		Asf1b		p60		p150		Ki67	
	N	p-value	N	p-value	N	p-value	N	p-value	N	p-value
Clinicopathological factors										
Age		0.70		0.36		1.0		0.79		**4.7x10-3**
<=50	34		53		44		53		53	
>50	21		32		31		33		33	
Tumor size		0.06		**6.3x10-3**		**0.028**		0.34		**6.6x10-3**
no tumor/T1a	33		53		46		53		53	
T2a	22		32		29		33		33	
Pathological Tumor size		0.13		**2.1x10-4**		0.07		0.17		**0.013**
<=20 mm	38		59		51		59		59	
>20 mm	17		26		24		27		27	
Number of mitosis		0.07		**6.3x10-6**		**1.4x10-3**		**1.2x10-3**		**2.3x10-4**
<=10	31		53		44		53		53	
>10	24		32		31		33		33	
Grade EE		0.06		**1.2x10-6**		**9.5x10-3**		**0.04**		**5.4x10-5**
I	18		29		25		29		29	
II	24		34		29		35		35	
III	13		22		21		22		22	

	Asf1a		Asf1b		p60		p150		Ki67	
	r	p-value	r	p-value	r	p-value	r	p-value	r	p-value
Correlations with other markers										
CAF-1 p60	0.42	**2.5x10-3**	0.66	**2.4x10-10**	——		0.84	**p<2.2x10-16**	0.26	**0.026**
CAF-1 p150	0.53	**2.6x10-5**	0.64	**3.6x10-11**	0.84	**p<2,2x10-16**	——		0.21	0.054
Ki67	0.02	0.86	0.52	**3.6x10-7**	0.26	**0.026**	0.21	0.054	——	
Asf1a	——		0.32	**0.017**	0.42	**2.5x10-3**	0.53	**2.6x10-5**	0.02	0.86
Asf1b	0.32	**0.017**	——		0.66	**2.4x10-10**	0.64	**3.6x10-11**	0.52	**3.6x10-7**

Supplementary Table SIII. Multivariate analysis in patients of 1996

COX MODEL FOR METASTASIS FREE INTERVAL (n = 62)

Variables included in the model: mitotic index (qualitative), menopause status, ablation surgery quality, progesteron receptor status, Asf1b, Ki67

Variables		RR	95% CI	p-value
Asf1b	Asf1b < 0.3	1	-	-
	Asf1b ≥ 0.3	5.7	1.3 - 25.7	**0.024**
Menopaused		1	-	-
Non menopaused		4.2	1.4 - 12.8	**0.013**

COX MODEL FOR DISEASE FREE INTERVAL (n = 62)

Variables included in the model: mitotic index (qualitative), tumor size (qualitative), menopause status, Asf1b, CAF-1 p60, Ki67

Variables		RR	95% CI	p-value
Asf1b	Asf1b < 0.3	1	-	-
	Asf1b ≥ 0.3	3.24	1.2 - 8.5	**0.0163**
Menopaused		1	-	-
Non menopaused		2.59	1.1 - 6.2	**0.0322**

COX MODEL FOR OVERALL SURVIVAL (n = 62)

Variables included in the model: mitotic index (qualitative), ablation surgery quality, Asf1b, CAF-1 p60, Ki67

Variables		RR	95% CI	p-value
Ki67	Ki67 ≤ 40	1	-	-
	Ki67 > 40	6.18	1.6 - 24.0	**0.008**
Complete ablation surgery		1	-	-
Incomplete ablation surgery		4.0	1.0 - 15.4	**0.046**